IEEE Photonics Journal
An IEEE Photonics Society Publication

Experimental Demonstration of π Equivalent Phase-Shifted SBG Laser With Controlled Distributed Phase Shift

Volume 11, Number 6, December 2019

Rulei Xiao
Runze Liu
Yating Zhou
Zhenxing Sun
Jun Lu
Yuechun Shi
Xiangfei Chen

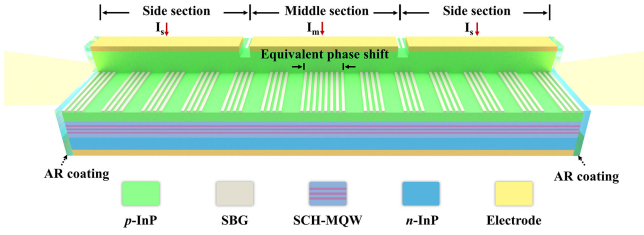

DOI: 10.1109/JPHOT.2019.2950672

IEEE photonics SOCIETY
IEEE

Experimental Demonstration of π Equivalent Phase-Shifted SBG Laser With Controlled Distributed Phase Shift

Rulei Xiao,[1,2,3,4] Runze Liu,[3] Yating Zhou,[1] Zhenxing Sun,[3] Jun Lu,[3] Yuechun Shi,[3] and Xiangfei Chen [3]

[1]School of Chemical Engineering and Materials, Changzhou Institute of Technology, Changzhou 213032, China
[2]Key Laboratory of Intelligent Optical Sensing and Manipulation of the Ministry of Education, Nanjing University, Jiangsu 210009, China
[3]National Laboratory of Solid State Microstructures and College of Engineering and Applied Sciences, Nanjing University, Jiangsu 210093, China
[4]Institute of Optical Communication Engineering, Nanjing University, Jiangsu 210093, China

DOI:10.1109/JPHOT.2019.2950672

Manuscript received August 18, 2019; revised October 20, 2019; accepted October 26, 2019. Date of publication October 31, 2019; date of current version December 16, 2019. This work was supported in part by the Chinese National Key Basic Research Special Fund under Grant 2017YFA0206401, in part by the Science and Technology Project and Natural Science Foundation of Jiangsu province under Grants BE2017003-2 and BK20160907, in part by the National Natural Science Foundation of China under Grants 61435014 and 11574141, and in part by Suzhou Technological innovation of key industries under Grant SYG201844. Corresponding author: Yating Zhou (e-mail: zhou-yating@163.com).

Abstract: We designed and fabricated a π equivalent phase-shifted sampled Bragg grating (SBG) semiconductor laser with a controlled distributed phase shift. The phase shift is equivalently realized with reconstruction-equivalent-chirp (REC) technique. The laser is divided into three sections with the same length. By injecting different currents into the side and middle sections, a distributed phase shift can be introduced. The lasing wavelength can be continuously tuned by the injection currents. In our experiment, when the total current keeps 130 mA, the lasing wavelength can be continuously tuned by 1.2 nm. During the tuning, the side mode suppression ratio keeps above 40 dB and the output power varies only 1.3 dB. Therefore, the proposed method provides an alternative solution for the multiwavelength laser arrays in dense wavelength-division multiplexing (DWDM) systems.

Index Terms: Semiconductor lasers, tunable lasers, fiber gratings.

1. Introduction

Semiconductor lasers have been widely applied as light sources in optical communication owing to its compact structure, low power consumption, low production cost, and high quantum efficiency [1]. Distributed feedback (DFB) semiconductor lasers are one kind of crucial light sources. It can lase at a stable wavelength with a good single-mode property [2]. With the explosive increase of data traffic in datacenters and backbone networks, the dense wavelength division multiplexing (DWDM) technology is invented and thought as a promising solution. The DWDM technology multiplies transmission bandwidth by tens of times in a single fiber [3]. The wavelength spacing between neighboring channels is as narrow as 100 or 50 GHz, corresponding to the wavelength step of 0.80 or 0.40 nm, respectively [4]. Therefore, high-precision control for the wavelength is required in the DWDM technology [5].

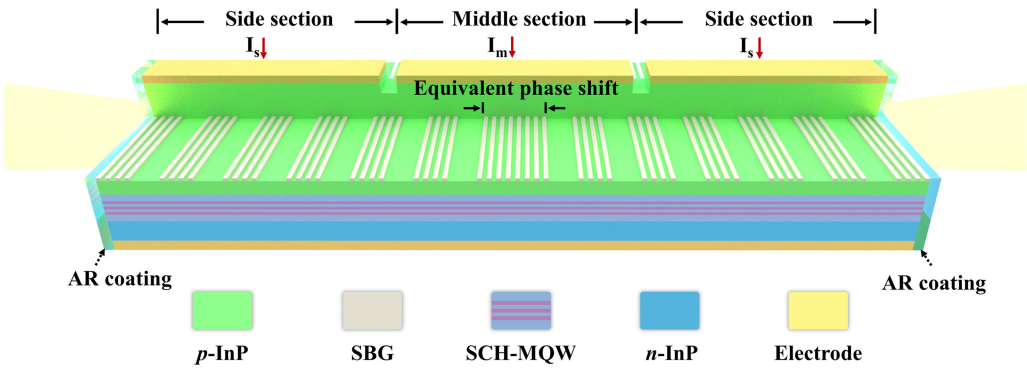

Fig. 1. Schematic of the proposed three-section DFB laser with a π equivalent phase shift. (AR: anti-reflection; SBG: sampled Bragg grating; SCH-MQW: separate-confinement heterostructure multi-quantum well).

In an actual DWDM system, the DFB laser array is a good candidate for the multiwavelength source, owing to its stable lasing wavelengths [6]. In a normal DFB laser, the wavelength is defined mainly by its grating period. To realize the wavelength variation of 0.80 nm, the grating period should be controlled to change only 0.025 nm approximately. Therefore, it is difficult to fabricate a DFB laser array with such wavelength precision. To solve this problem, it is reported that each DFB laser is typically fabricated attached with an individual thin-film heater, which tunes the lasing wavelength thermally [7].

In the past decade, the reconstruction equivalent chirp (REC) technique has been proposed to fabricate the DFB laser array. With the REC technique, phase shifts and grating chirps were equivalently realized on the basis of sampled Bragg gratings (SBGs) [8]–[10]. The lasing wavelengths are defined by the sampled periods where the seed grating keeps uniform. As a result, for the REC-based laser array, the wavelength spacing precision can be greatly improved [11]. As reported in Ref. [10], 60-wavelength DFB laser arrays have been demonstrated experimentally. The statistics of all 1600 lasers show that 83% lasers are within a wavelength deviation of 0.20 nm, and nearly all the lasers are within a wavelength deviation of 0.40 nm.

However, in the DWDM networks, the REC-based laser array still needs a fine-tuning mechanism to meet the frequency grid. In our previous study, we had designed and fabricated a three-section semiconductor laser with uniform SBG [12]. By injecting different currents into the middle and side sections, a distributed phase shift (DPS) can be introduced. By tuning the current injections, the DPS can vary in cycles, and the lasing wavelength can change in the stopband. Under the constant total current of 150 mA, the lasing wavelength can be tuned continuously by about 1.1 nm. During the tuning, the side mode suppression ratio (SMSR) keeps above 40 dB, while the output power varies 1.4 dB.

To explore the influence of the DPS in a DFB laser on the lasing properties, this paper studied a three-section REC-based DFB laser by simulations and experiments. Our experimental results show that, when the total current keeps 130 mA, the lasing wavelength can be tuned continuously by 1.2 nm. At the same time, the SMSRs keep above 40 dB and the output power fluctuates only 1.3 dB.

2. Device Structure and Simulation Study

2.1. Device Fabrication

As shown in Fig. 1, the studied laser mainly consists of four layers—an n-type InP contact layer, a grating layer, a separate confinement heterostructure multi-quantum well layer, and a p-type InP contact layer. Layers with different components are grown on the InP substrate by the metal-organic chemical vapor deposition technology. The equivalent phase-shifted sampled Bragg grating

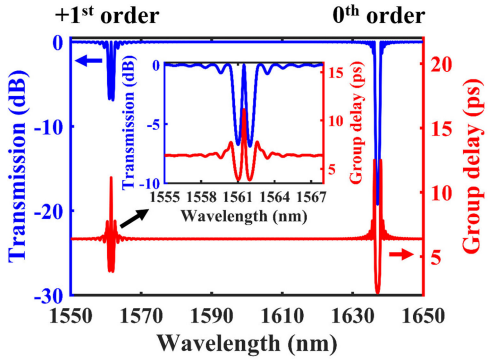

Fig. 2. Simulated transmission and group delay spectra of the equivalent phase-shifted sampled Bragg grating.

is defined by two steps of exposure, one holography exposure, and one sampled pattern mask exposure, and then etched by inductively coupled plasma etching. A ridge-type waveguide is formed by mask exposure and inductively coupled plasma etching. Electrical isolation between these three sections is enabled by shallow-etched grooves. Ti/Pt/Au metal layers are deposited as p- and n-electrodes by magnetron sputtering. The lift-off technique is used to define the electrode shape. Thermal annealing is then applied to improve metal contact and lower electrical resistance. Then laser diodes are obtained after cleaving, and two cleaved facets are coated with silicon oxide layer for anti-reflection and protection.

2.2. REC Technique

The $+$1st order channel of the sampled Bragg grating is the lasing channel and designed around 1560 nm in the center of the material gain. The 0th order Bragg wavelength is 1635 nm where the material gain can be negligible. The relation between the grating period and sampled period is given by

$$\frac{1}{\Lambda_{+1}} = \frac{1}{\Lambda_0} + \frac{1}{P}. \tag{1}$$

Here, Λ_{+1} is the equivalent grating period of the $+$1st order channel, Λ_0 is the grating period, and P is the sampled period [13]. Noted that the period Λ_{+1} is not a physical grating period, but a period component by Fourier transform of the sampled grating superlattice. Phase shifts can be equivalently realized by introducing a defect into the sampled pattern. For example, to achieve a π phase shift, the defect size (ΔP) should be $P/2$ according to Eq. 2, where φ_{+1} is the equivalent phase shift in the $+$1st order grating. The Bragg wavelength of the $+$1st order channel λ_{+1} is given in Eq. 3, where n is the effective refractive index.

$$\varphi_{+1} = 2\pi \frac{\Delta P}{P}. \tag{2}$$

$$\lambda_{+1} = 2n\Lambda_{+1}. \tag{3}$$

The total cavity length of the proposed laser structure is 600 μm which is equally divided into three sections. In our investigation, n is about 3.185 without injection current. $\wedge_0$ and P were designed as 257 nm and 5.3 μm, respectively. By using the transfer matrix method, transmission and group delay spectra were calculated, as shown in Fig. 2. The 0th and $+$1st order channels locate at 1635 nm and 1560 nm, respectively. A π equivalent phase shift was implemented into the $+$1st order channel, as shown in the inset of Fig. 2.

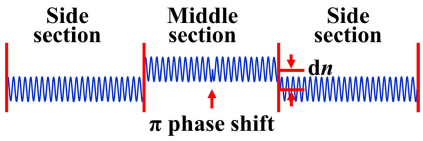

Fig. 3. Schematic of the proposed π phase-shifted Bragg grating where a DPS is introduced by the refractive index difference dn.

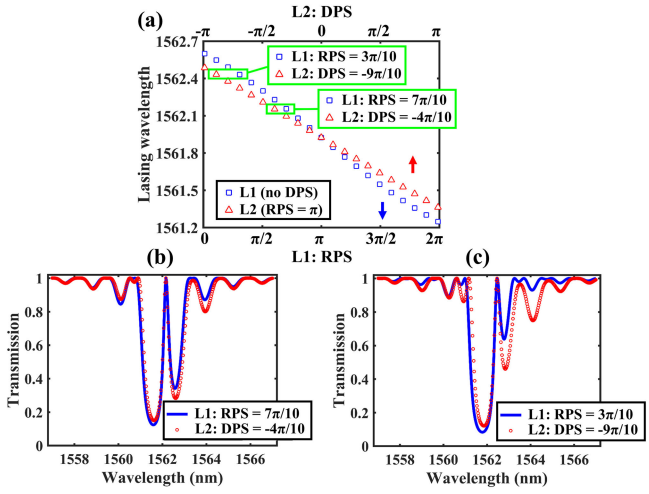

Fig. 4. (a) Simulated lasing wavelengths vary with RPS in L1 and DPS in L2. (b) Simulated transmission spectra of L1 where RPS $= 7\pi/10$ and L2 where DPS $= -4\pi/10$. (c) Simulated transmission spectra of L1 when RPS $= 3\pi/10$ and L2 when DPS $= -9\pi/10$.

2.3. Wavelength Tuning Simulation

In our work, the same currents were injected into the two side sections. When different currents are injected into the middle and side sections, an effective refractive index difference Δn is introduced. Therefore, a distributed phase shift (DPS) is introduced, as defined by [14]

$$DPS = \frac{2\pi \Delta n L_m}{n\Lambda_{+1}}. \tag{4}$$

Here, L_m is the length of the middle section. The refractive index difference Δn is changed by the injected current due to the thermal effect and free-carrier plasma effect [15]. Therefore, the DPS is introduced by different current injections into the three sections. According to our previous studies, the REC-based equivalent phase-shifted laser has similar performance with the RPS laser. Therefore, an RPS laser is substituted for an equivalent phase-shifted laser in simulation for simplification.

In our simulations, two tuning mechanisms are studied for comparison: one is the wavelength tuning by changing the real phase shift (RPS) of a DFB laser where no DPS is introduced; the other one is the wavelength tuning by the DPS of a π phase-shifted DFB laser, as shown in Fig. 3. For convenience, these two situations of lasers are abbreviated as L1 and L2. L1 refers to a laser whose RPS is changed with no DPS, and L2 refers to that DPS is changed with RPS fixed at π.

With the increase of RPS and DPS for the L1 and L2, respectively, the lasing wavelengths all decrease, as seen in Fig. 4. We can also find that, even if the value of the RPS in L1 is equal to the sum of the DPS and RPS in L2, the L1 and L2 have a different lasing wavelength. That is to say, the RPS and DPS have different influences on the lasing wavelengths. In our study, we analyzed the threshold condition of the L1 and L2. Here, the total length of the laser cavity is 600 μm and divided into three sections with the same length. The effective refractive index is 3.185 at 1550 nm,

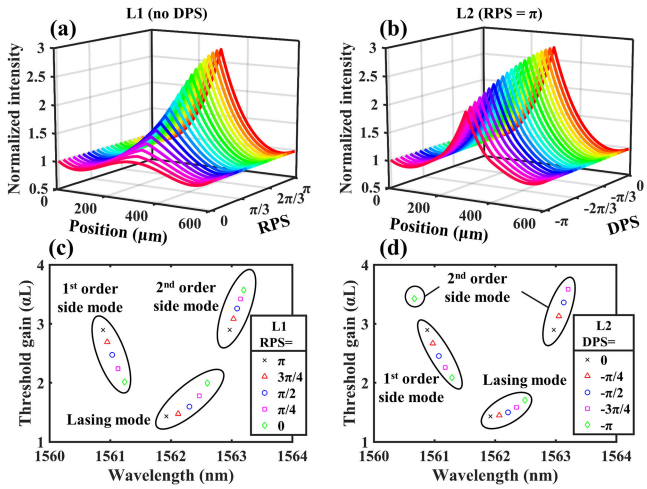

Fig. 5. Simulated photon intensity distributions along the grating cavities in (a) L1 and (b) L2. Simulated threshold gain of different modes in (c) L1 under different RPS and (d) L2 under different DPS. Here, the 1st order side mode refers to the most probable lasing side mode, and the 2nd order side mode refers to the second probable lasing side mode.

and the grating period is 245.4 nm. In Fig. 4, the DPS in L2 varied from $-\pi$ to π are introduced by a refractive index difference from -0.0025 to 0.0025 between the middle and side sections.

In our views, the optical path difference induced the resonating wavelength shift, which is why the lasing wavelength can be tuned. Similar to that in Ref. [12], with the variation of RPS or DPS, the lasing wavelength can be tuned back and forth inside the grating stop-band. As shown in Fig. 4(a), the lasing wavelength of L1 can be tuned from 1561.25 to 1562.60 nm within 1.35 nm variation, and that of L2 from 1561.36 to 1562.49 nm within 1.13 nm variation. The L1 and L2 can have the same lasing wavelength. As seen in Fig. 4(a) to (c), when RPS in L1 is $7\pi/10$ and DPS in L2 is $-4\pi/10$, L1's lasing wavelength is equal to L2's. Meanwhile, their transmission spectrum is similar to each other. Such situations can also be seen when the RPS in L1 is $3\pi/10$ and DPS in L2 is $-9\pi/10$.

In our study, we studied the power intensity distribution along the laser cavity in where the total output power is normalized as 1. As shown in Fig. 5(a), when RPS in L1 is π, there is a resonating peak in the center of the laser cavity. When the RPS is changed from π to 0, the resonating peak gradually disappears. Fig 5(b) shows when DPS in L2 is 0, there is also a resonating peak in the center of the laser cavity. But when the DPS is changed from 0 to $-\pi$, the resonating peak still exists but slightly decays. Figures 5(c) shows the threshold gains of the lasing mode, 1st and 2nd order side modes in L1 when PS is varied from π to 0. Noted that the lasing mode refers to the most probable lasing mode and will lase in normal condition. The 1st order side mode refers to the most probable lasing side mode, which will not lase in normal condition but may lase when a large current is applied. The threshold gain of the 1st order side mode has an important influence on the single-mode property of the laser. The 2nd order side mode refers to the second probable lasing side mode. When the RPS approaches 0 in L1, the gain margin between the lasing mode and the 1st order side mode also approaches 0, which indicates the poor single-mode property. Fig. 5(d) shows when the DPS is changed from 0 to $-\pi$ in L2, the gain margin decreases but keeps larger than 0.3, which indicates under such situations L2 still has good single-mode property.

Figure 6 shows the lasing wavelength, $+1$st order side mode, and gain margin when the DPS is varied from -2π to 2π in L2. When the DPS is 0, the highest gain margin is obtained, which corresponds to the best single-mode property. When the absolute value of the DPS is increased from 0 to 2π, the gain margin drops and subsequently rises. When the DPS is $\pm 4\pi/3$ the gain margin is near 0, while the mode hopping happens. Generally, a DFB laser has good single-mode property when the gain margin is larger than 0.25. Our simulation shows L2 has good single-mode properties except when the DPS is near $\pm 4\pi/3$. Under single-mode operation, its lasing wavelength can be continuously tuned by about 1.3 nm.

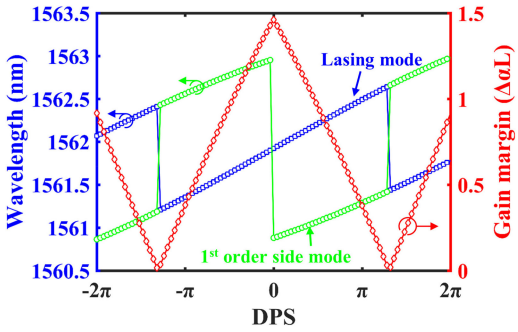

Fig. 6. Simulated wavelengths of the lasing mode and 1st order side mode in L2. Simulated gain margin ($\Delta\alpha L$) when the DPS is varied from -2π to 2π in L2.

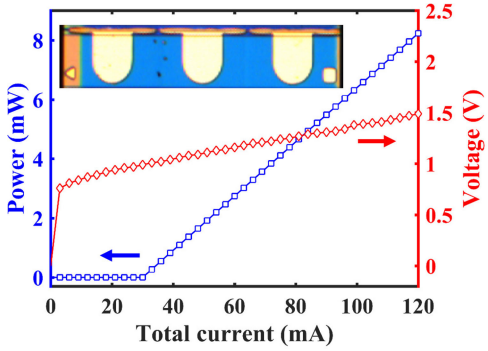

Fig. 7. Measured output power and voltage applied to the studied laser when the same currents injected into its three electrodes. The total current is varied from 0 to 120 mA. The inset is an optical micrograph of the measured laser.

As a matter of fact, when L1's RPS is near 0 or 2π, L1 will operate on dual-mode. Under single-mode operation, theoretical calculation shows L1's lasing wavelength can also be continuously tuned by about 1.3 nm. That is to say, L1 and L2 have similar operation performance.

3. Device Measurement

In our measurement, the studied π equivalent phase-shifted DFB laser was mounted on a sub-mount, whose temperature was controlled at 20 °C by a thermal electronic cooler. The optical spectra were recorded by the AQ6370 optical spectrum analyzer. As shown in Fig. 7, when the studied laser was injected the same currents into its three sections, the lasing output power and voltage applied on its electrodes were recorded. The inset in Fig. 7 is an optical micrograph of the fabricated laser chip. The threshold current is 30.0 mA, and the slope efficiency is approximately 0.091 W/A. The series resistance is approximately 5.33 Ω when the total current is 60.0 mA.

In this paper, to simplify expression the currents are injected into the two side sections are named as *I*s, while that into the middle section is named as I_m. When $I_s \neq I_m$, between the side sections and the middle section, an effective refractive index difference is introduced. And then a DPS is introduced into the studied laser.

In our measurement, to the begin I_s was set to be constant at 40 mA and I_m was tuned from 0 to 120 mA. Fig. 8(a) to (c) shows the studied laser's optical spectra, lasing wavelengths, and SMSRs, as well as output under such situations. From Fig. 8 it can be seen when I_m was tuned from 19 to 88 mA, the SMSRs are both larger than 40 dB and the output increases from 7.7 to 9.8 dBm. The laser keeps good single-mode operation and its lasing wavelength varies from 1,562.0 to 1564.6 nm

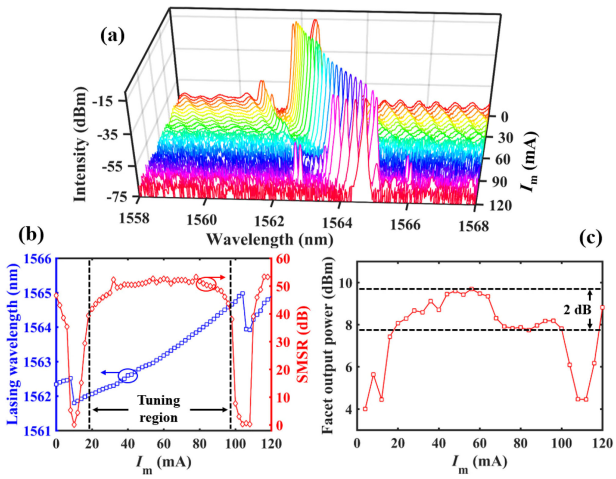

Fig. 8. At 20 °C when I_s = 40 mA, I_m is tuned from 0 to 120 mA, the measured (a) spectra, (b) wavelengths and SMSRs, (c) output power of the studied laser. (SMSR: side-mode suppression ratio).

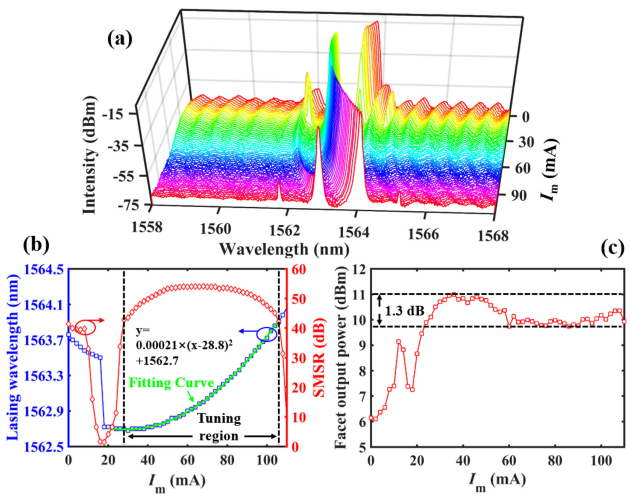

Fig. 9. Measured (a) lasing spectra, (b) lasing wavelengths and SMSRs, and (c) output power when I_m is varied from 0 to 110 mA. The total current, $I_m + 2I_s$, keeps 130 mA. The ambient temperature is controlled at 20 °C (SMSR: side-mode suppression ratio).

which refers to a continuous tuning range of 2.6 nm. It is found that the lasing wavelength can be tuned as nearly twice as the calculated result. The reason is that with the increase of I_m, more Joule heat accumulation and diffusion along the lasing cavity. The Joule heat accumulation causes the temperature of the laser chip to increase. Hence the effective refractivity index of the whole laser cavity increases. It can also be found that the lasing wavelength changes almost linearly with the variation of I_m and the slope is 0.0377 nm/mA. When the I_m is near 10 or 105 mA around, it can be found the SMSRs become very low and almost zero. The phenomenon is consistent with the theoretical analyses when DPS in L2 equals to $\pm 4\pi/3$, as seen in Fig. 6.

In order to reduce the fluctuation of output, it is expected the total current injected into the studied laser keeps constant. In our experiment, the constant current, $I_m + 2I_s$, is selected to be 130 mA. When I_m increases from 0 to 110 mA, I_s decreases from 65 to 10 mA. Fig. 9(a) to (c) shows the optical spectra, lasing wavelengths, and SMSRs, as well as output of the studied laser when I_m+2I_s

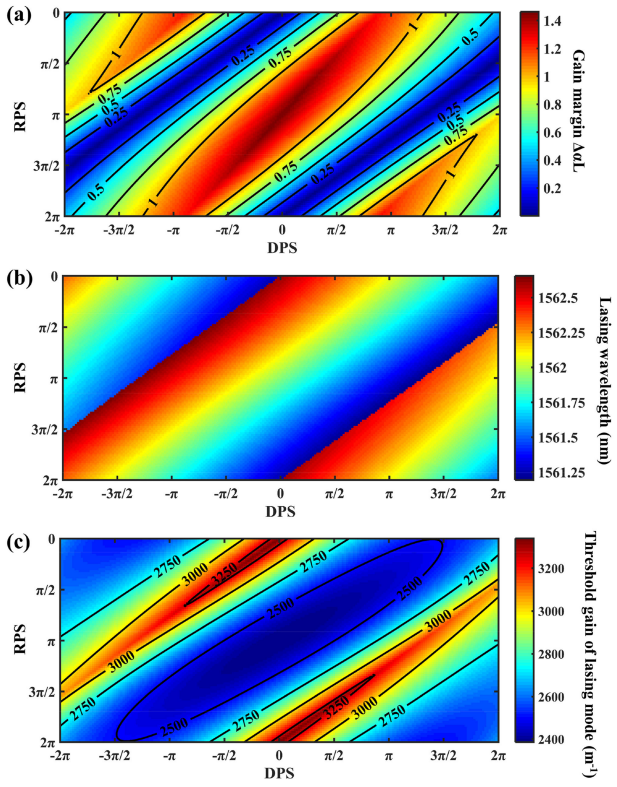

Fig. 10. Simulated (a) gain margin, (b) lasing wavelength, and (c) threshold gain of lasing mode when the RPS is varied from 0 to 2π and the DPS is varied from -2π to 2π.

keep 130 mA. It can be seen when I_m was tuned from 27 to 106 mA, the SMSRs are both larger than 40 dB and the output increases from 9.7 to 11.0 dBm. The fluctuation of output is only 1.3 dB, and the laser keeps in good single-mode operation. Its lasing wavelength varies from 1,562.7 to 1563.9 nm while the lasing wavelength can be continuously tuned by 1.2 nm. With the increase of I_m, the wavelength increases with a parabolic tendency. When the whole current $I_m + 2I_s$ is constant, the effective refractive index difference between the middle and side sections varies with the I_m parabolically. In Fig. 9(b), the quadratic coefficient of 0.00021 is obtained after parabolic fitting.

4. Discussions

We further simulated the performance of the laser where the RPS and DPS coexist and varies simultaneously. The gain margin ($\Delta\alpha L$), lasing wavelength, and threshold gain are studied when the DPS is varied from -2π to 2π, and the PS is varied from 0 to 2π. As shown in Fig. 10(a), the highest gain margin is obtained when DPS $= 0$ and RPS $= \pi$, which is the widely-used π phase-shifted laser in existing DWDM networks. The gain margin decays rapidly when the DPS is fixed at 0 and the RPS is changed away from π. The same situations can be observed when the RPS is fixed at π and the DPS is changed away from 0. The gain margin keeps large when the PS and the DPS are changed oppositely. Lowest gain margin near zero is observed when the summation of $0.75\times$DPS and PS equals to 0 or 2π. As shown in Fig. 10(b), when the RPS or DPS is increased, the lasing wavelength is decreased linearly except for the near-zero gain margin where mode hopping occurs. The threshold gain of lasing mode has a positive correlation with the threshold current of the laser. By comparing Fig. 10(a) and (c), it is found that the threshold gain is low when the gain margin is high and vice versa.

5. Conclusions

In summary, a π equivalent phase-shifted DFB laser, which has three sections with the same length, was studied by simulation and experiment. By injecting different currents into its middle and side sections, a DPS is introduced into the studied laser. To change the currents injected into the middle section and side sections, the DPS can be controlled and then the lasing wavelength can be tuned. When the currents to the side sections are 40 mA and that to the middle section varies from 19 to 88 mA, the SMSRs keep above 40 dB. At the same time, the lasing wavelength can be continuously tuned by 2.6 nm while the output varies 2.2 dB. When the current is injected into the whole laser keeps 130 mA and the current into the middle section was tuned from 27 to 106 mA, the lasing wavelength can be continuously tuned by 1.2 nm while the output varies only 1.3 dB. Because the studied laser has good single-mode property and can tune the wavelength to meet ITU-T standard, it is a good candidate for the multiwavelength laser array in the future DWDM system.

References

[1] N. K. Dutta, "Long-wavelength semiconductor lasers," in *Proc. Tech. Digest., Int. Electron Devices Meeting*, 1988, pp. 304–306.

[2] R. Tkach and A. Chraplyvy, "Regimes of feedback effects in 1.5-μm distributed feedback lasers," *J. Lightw. Technol.*, vol. 4, no. 11, pp. 1655–1661, Nov. 1986.

[3] C. A. Brackett, "Dense wavelength division multiplexing networks: Principles and applications," *IEEE J. Sel. Areas Commun.*, vol. 8, no. 6, pp. 948–964, Aug. 1990.

[4] S. Chandrasekhar and X. Liu, "Impact of channel plan and dispersion map on hybrid DWDM transmission of 42.7-Gb/s DQPSK and 10.7-Gb/s OOK on 50-GHz grid," *IEEE Photon. Technol. Lett.*, vol. 19, no. 22, pp. 1801–1803, Nov. 2007.

[5] R. Nagarajan *et al.*, "Large-scale photonic integrated circuits," *IEEE J. Sel. Top. Quantum Electron.*, vol. 11, no. 1, pp. 50–65, Jan. 2005.

[6] L. J. P. Ketelsen *et al.*, "Multiwavelength DFB laser array with integrated spot size converters," *IEEE J. Quantum Electron.*, vol. 36, no. 6, pp. 641–648, Jun. 2000.

[7] H. Hillmer and B. Klepser, "Low-cost edge-emitting DFB laser arrays for DWDM communication systems implemented by bent and tilted waveguides," *IEEE J. Quantum Electron.*, vol. 40, no. 10, pp. 1377–1383, Oct. 2004.

[8] Y. Dai and X. Chen, "DFB semiconductor lasers based on reconstruction-equivalent-chirp technology," *Opt. Exp.*, vol. 15, no. 5, pp. 2348–2353, 2007.

[9] Y. Shi *et al.*, "Experimental demonstration of eight-wavelength distributed feedback semiconductor laser array using equivalent phase shift," *Opt. Lett.*, vol. 37, no. 16, pp. 3315–3317, 2012.

[10] Y. Shi *et al.*, "High channel count and high precision channel spacing multi-wavelength laser array for future PICs," *Sci. Rep.*, vol. 4, 2014, Art. no. 7377.

[11] Y. Shi *et al.*, "Study of the multiwavelength DFB semiconductor laser array based on the reconstruction-equivalent-chirp technique," *J. Lightw. Technol.*, vol. 31, no. 20, pp. 3243–3250, Oct. 2013.

[12] R. Guo *et al.*, "Experimental demonstration of SBG semiconductor laser with controlled phase shift," *IEEE Photon. Technol. Lett.*, vol. 29, no. 1, pp. 126–129, Jan. 2017.

[13] Y. Dai, X. Chen, L. Xia, Y. Zhang, and S. Xie, "Sampled Bragg grating with desired response in one channel by use of a reconstruction algorithm and equivalent chirp," *Opt. Lett.*, vol. 29, no. 12, pp. 1333–1335, 2004.

[14] M. Tohyama, M. Onomura, M. Funemizu, and N. Suzuki, "Wavelength tuning mechanism in three-electrode DFB lasers," *IEEE Photon. Technol. Lett.*, vol. 5, no. 6, pp. 616–618, Jun. 1993.

[15] V. Paschos, T. Sphicopoulos, D. Syvridis, and C. Caroubalos, "Influence of thermal effects on the tunability of three-electrode DFB lasers," *IEEE J. Quantum Electron.*, vol. 30, no. 3, pp. 660–667, Mar. 1994.